Measurements of the Deuteron Elastic Structure Function A(Q^2) at the Jefferson Laboratory

J. Gomez* †

Thomas Jefferson National Accelerator Facility, Newport News, Va, USA

Abstract. The deuteron elastic structure function $A(Q^2)$ has been extracted in the range $0.7 \leq Q^2 \leq 6.0$ (GeV/c)^2 from cross section measurements of elastic electron-deuteron in coincidence.

Measurements of the elastic deuteron electromagnetic form factors offer unique opportunities to test models of short-range aspects of the nucleon-nucleon interaction, meson-exchange currents, isobaric configurations and, quark degrees of freedom. The elastic electron-deuteron cross section is given by $d\sigma/d\Omega = \sigma_M \left[A(Q^2) + B(Q^2)\tan^2(\theta/2)\right]$ where θ is the electron scattering angle, $\sigma_M = \alpha^2 E' \cos^2(\theta/2)/[4E^3 \sin^4(\theta/2)]$ is the Mott cross section, α is the fine-structure constant, E and E' are the incident and scattered electron energies and $Q^2 = 4EE' \sin^2(\theta/2)$ is the four-momentum transfer squared. The deuteron elastic structure functions $A(Q^2)$ and $B(Q^2)$ are given in terms of the charge, quadrupole and magnetic form factors $F_c(Q^2)$, $F_q(Q^2)$ and $F_m(Q^2)$ by $A(Q^2) = F_c^2(Q^2) + (8/9)\tau^2 F_q^2(Q^2) + (2/3)\tau F_m^2(Q^2)$ and $B(Q^2) = (4/3)\tau(1+\tau)F_m^2(Q^2)$ with $\tau = Q^2/4M_d^2$. M_d is the deuteron mass. The aim of the experiment reported here was to extend the previously measured kinematical range of $A(Q^2)$ and to resolve inconsistencies in previous data sets [1, 2, 3] by measuring elastic electron-deuteron (e-d) cross sections for $0.7 \leq Q^2 \leq 6.0$ (GeV/c)^2.

The experiment was conducted in one of the experimental areas (Hall A) of the Thomas Jefferson National Accelerator Facility (JLab). Incident electron beams with energies from 3.2 to 4.4 GeV, currents from 5 to 120 μA and, 100% duty-factor were used in this experiment. Beam current and energy uncertainties were estimated to be ±2% and ±0.2%, respectively. Uncertainties due to beam position and angle at the target are negligible. The target system consisted of two 15 cm long cylindrical cells: one filled with liquid hydrogen, the other with liquid deuterium. Measured beam-induced density changes were

---

**Representing the JLab Hall A collaboration.*

†*E-mail address:* gomez@jlab.org

~2% at 120 μA. A 15 cm long "empty" target was used to measure possible contributions from the full cell end-caps to the measured cross sections. They were found to be negligible.

The Hall A experimental facility at JLab consists of two, magnetically identical, QQDQ High Resolution Spectrometers (HRS) of 4 GeV/c maximum momentum. One HRS deflected negatively charged particles into the focal plane (electron HRS) while the other was set for positive particles (recoil HRS). Both HRS have two planes of plastic scintillators for triggering and timing and a pair of drift chambers for track reconstruction. In addition, the electron HRS has a gas Čerenkov and a Pb-glass calorimeter for electron identification. The trigger logic was set to accept all electron-recoil spectrometer coincidences as well as samples of single-arm triggers (for detector efficiency studies). The coincidence trigger efficiency ranged from 98% to 100%.

Coincidence elastic electron-proton (e-p) cross sections were measured in this experiment to check our understanding of spectrometer optics and double-arm acceptance. The e-p kinematics were selected such that the electron-recoil solid angle jacobian for e-p was the same as for e-d. The e-p data were taken with and without solid-angle defining collimators in front of the spectrometers.

In the data analysis, electron events were required to have a minimum pulse height in the Čerenkov counter and energy deposition in the calorimeter consistent with the momentum determined from the drift chamber track. Coincident events were identified using the relative time-of-flight (TOF) between the electron and recoil triggers. Contributions from random coincidences were in general negligible.

The elastic e-p and e-d cross sections were calculated according to $d\sigma/d\Omega = N_{ep(ed)} C_{eff}/[N_i N_t F\ \Delta\Omega]$ where $N_{ep(ed)}$ is the number of e-p(e-d) elastic events, N_i is the number of incident electrons, N_t is the number of target nuclei/cm^2, $\Delta\Omega$ is the effective double-arm solid angle including the spectrometer acceptance-dependent part of the radiative corrections, F is the portion of the radiative corrections that depends only on Q^2 and target thickness, and C_{eff} is the product of corrections such as detector and trigger inefficiency in both electron and recoil spectrometers (1-3%), computer dead time (typically 5%) and, proton (~2%) and deuteron (~4%) absorption losses in the target and detectors.

The effective double-arm solid angle $\Delta\Omega$ was evaluated with a Monte Carlo computer program that simulated elastic e-p and e-d scattering under identical conditions as our measurements. The program ray-traced scattered electrons and recoil nuclei from the target to the detectors through models representing the magnetic characteristics, physical apertures and alignment of each HRS. The effects from ionization energy losses and multiple scattering in the target and vacuum windows were taken into account for both electrons and recoil nuclei. Bremsstrahlung radiation losses for both incident and scattered electrons in the target and vacuum windows as well as internal radiative effects were also taken into account. Details on this simulation method can be found in ref. [4].

The measured elastic e-p cross sections, with and without collimators, agree within $\pm$6% with the values calculated from a recent parametrization [5] of proton world data. Values of $A(Q^2)$ were then extracted from the measured

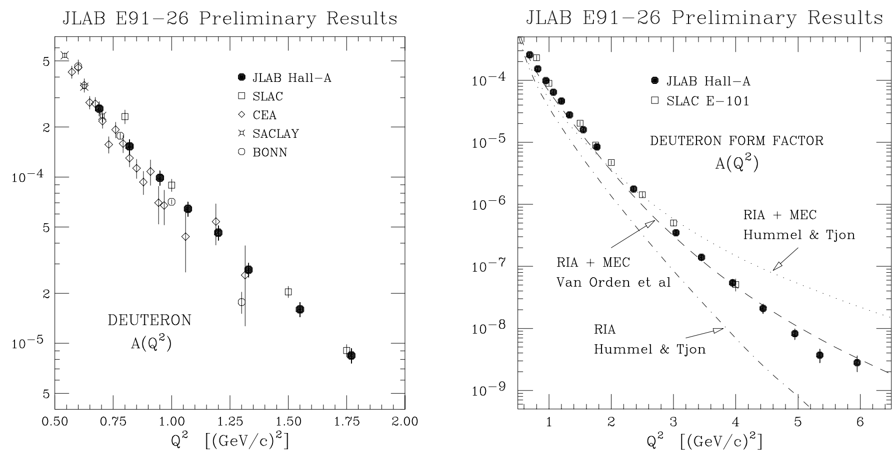

Figure 1. The left panel shows our data in the "low" Q^2 region. The previous measurements tend to show two long-standing diverging trends, one supported by the SLAC data [2] and the other by the CEA [1] and Bonn [3] data. Our data confirm the trend of the SLAC data. The right panel shows all of our data together with previous SLAC data. The two data sets agree well in the range of overlap. Our data continue to exhibit a smooth fall-off with Q^2. Theoretical calculations by Van Orden, Devine and Gross (VDG) [6] and Hummel and Tjon (HT) [7] are also shown. In the HT case, relativistic impulse approximation (RIA) calculations with and without meson-exchange currents (MEC) are shown. Clearly, at large Q^2, the RIA calculation alone lacks enough strength to account for the data, and the model becomes very sensitive to the inclusion of MEC. In the HT model, the $\rho\gamma\pi$ and $\omega\varepsilon\gamma$ MEC are included with form factors given by the Vector Dominance Model (VMD). Although not shown, the VDG model has a similar behavior: the RIA alone lacks enough strength, and inclusion of a $\rho\gamma\pi$ MEC with VMD form factors overshoots the data. The VDG model shown includes a $\rho\gamma\pi$ MEC with form factors given by quark models [8, 9].

e-d cross sections under the assumption that $B(Q^2)$ does not contribute in any sizable way to the cross sections (supported by the existing $B(Q^2)$ data). The extracted $A(Q^2)$ values are presented in Figs. 1 and 2. The error bars represent statistical and systematic uncertainties added in quadrature. The statistical error ranged from $\pm 1\%$ to $\pm 30\%$. The systematic error has been estimated to be $\sim \pm 8\%$ and is dominated by the uncertainty in the double-arm solid angle ($\pm 6\%$).

In summary, we have measured the elastic deuteron structure function $A(Q^2)$ in the range $0.7 \leq Q^2 \leq 6$ (GeV/c)^2. The results have clarified inconsistencies in previous low Q^2 data. The precision of our data will provide severe constraints on theoretical calculations of the electromagnetic structure of the two-body nuclear system. The results are consistent with meson-nucleon calculations based on the relativistic impulse approximation augmented by meson-exchange currents (although with softer form factors than those obtained from the VMD model). The results are also consistent with predictions

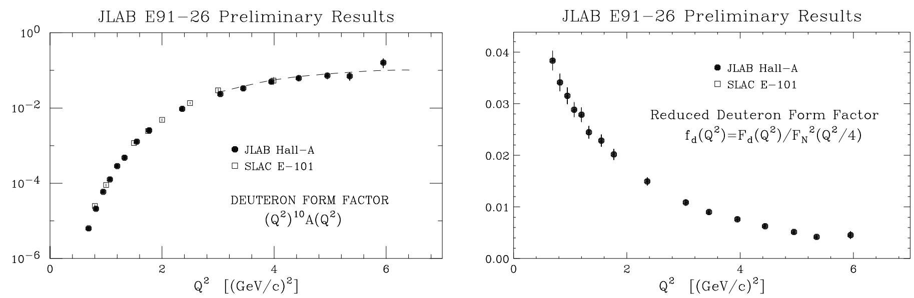

Figure 2. Deuteron models based on dimensional scaling [10, 11] and perturbative QCD [12] expect the "deuteron form factor" $F_d(Q^2)$ ($\equiv \sqrt{A(Q^2)}$) to fall as $(Q^2)^{-5}$. Consequently, the quantity $A(Q^2)\times(Q^2)^{10}$ should scale. Our data exhibits a scaling behavior compatible with those expectations (left panel). The right panel shows values for the "reduced" deuteron form factor $f_d(Q^2) \equiv F_d(Q^2)/F_N^2(Q^2/4)$ where the two powers of the nucleon form factor $F_N(Q^2) = (1 + Q^2/0.71)^{-2}$ remove in a minimal way the effects of nucleon structure [13].

of dimensional quark scaling and perturbative QCD. Future $A(Q^2)$ and $B(Q^2)$ measurements would be crucial for testing the apparent scaling behavior at large Q^2.

References

1. J.E. Elias et al.: Phys. Rev. **177**, 2075 (1969)
2. R.G. Arnold et al.: Phys. Rev. Lett. **35**, 776 (1975)
3. R. Cramer et al.: Z. Phys. **C29**, 513 (1985)
4. A.T. Katramatou et al.: Nucl. Instr. Meth. **A267**, 448 (1988)
   A.T. Katramatou: SLAC-NPAS-TN-86-08, 1986 (unpublished)
5. P.Y. Bosted: Phys. Rev. **C51**, 409 (1995)
6. J.W. Van Orden, N. Devine and F. Gross: Phys. Rev. Lett. **75**, 4369 (1995)
7. E. Hummel and J.A. Tjon: Phys. Rev. **C42**, 423 (1990)
8. K.L. Mitchell: PhD thesis, Kent State University, 1995 (unpublished)
9. F. Cardarelli et al.: Phys. Lett. **B359**, 1 (1995)
10. S.J. Brodsky and G.R. Farrar: Phys. Rev. Lett. **31**, 1153 (1973)
11. V. Matveev et al.: Nuovo Cimento Lett. **7**, 719 (1973)
12. S.J. Brodsky et al.: Phys. Rev. Lett. **51**, 83 (1983)
13. S.J. Brodsky and B.T. Chertok: Phys. Rev. Lett. **37**, 269 (1975)